Journal of Applied Polymer Science

Structure and properties of polylactide toughened by polyurethane prepolymer

Xu Zhang, Ernest Koranteng, Zhengshun Wu, Qiangxian Wu
Green Polymer Laboratory College of Chemistry, Central China Normal University, Wuhan, China 430079
Correspondence to: Q. Wu (E-mail: greenpolymerlab@yahoo.com)

ABSTRACT: In this study, polyurethane prepolymer (PUP) was prepared by the reaction of Poly-1,4-butylene glycol adipate diol (PBA) and 4,4′-Methylenedi-*p*-phenyl diisocyanate (MDI). The as-prepared PUP was then blended with Polylactide (PLA), and the impact of the PUP on the blends regarding their structure and properties were thoroughly analyzed. Also, PLA was blended with PU powder without isocyanate groups (NCO) as an important control sample (PLAPW) to study the interface interaction of the blends. Obvious yield and neck stretch were obtained after the addition of PUP, and the elongation ratio at break increased from 2.9% to 231.5%. In contrast, the mechanical properties of PLAPW decreased significantly mainly due to the simple physical blending of the polymers without the formation of covalent bonds. Also, the results of the FTIR, SEM, DSC, and DMA analysis showed that the reactions of NCO groups in PUP with the terminal hydroxyl or carboxyl groups in PLA significantly improved the compatibility of the PUP and PLA blend. Compared to pristine PLA, the highest decomposition temperature of the PLA and PUP blend (PLAPU) increased from 359.3°C to 362.6°C. Additionally the thermal stability and mechanical properties of the blended materials were exceedingly improved even with only 5% of PUP in the blended materials. © 2015 Wiley Periodicals, Inc. J. Appl. Polym. Sci. **2016**, *133*, 42983.

KEYWORDS: plasticizer; polyurethanes; thermal properties

Received 19 June 2015; accepted 25 September 2015
DOI: 10.1002/app.42983

INTRODUCTION

In recent years, biobased and biodegradable polymers, especially those derived from renewable resources have attracted considerable attention owing to the increased environmental concerns and the shortage of the traditional petroleum-based polymers.[1–3] Polylactide (PLA) is one of the most extensively investigated biobased and biodegradable polymers which has extensive potential in renewable resource applications such as biomedical materials, packaging, and in the automotive industries.[4–7] However, the diverse applications of PLA as a commodity polymer have been significantly restricted because of its inherent brittleness evidenced by a short elongation at break. Therefore, many approaches have been used to improve the toughness of PLA. Among them, polymer blending provides an economical and a practical way. For example, Poly (oxymethylene),[8] poly (ε-caprolactone),[9,10] poly (vinyl alcohol),[11] poly (ethylene glycol),[12] polyurethane,[13] poly (butylenes adipate-*co*-terephthalate),[14] bioelastomer,[15] poly (butylene succinate),[16] and thermoplastic polyurethane elastomer[17,18] have been used to blend with PLA to improve its toughness. Unfortunately, most of these polymers are immiscible with PLA, and studies have also indicated that these blended materials are unstable.[19] Thus, high-performance blended materials cannot be obtained by simple blending.

Polymer blends with excellent properties could be obtained by reactive blending of PLA and biopolymers with multiple reactive functional groups such as hydroxyl and carboxyl groups.[14] Therefore, reactive blending is a more effective method to prepare high-performance polymer blends than those obtained by simple blending because the compatibility of the component polymers can easily be improved by *in situ* reactions.[20–22] Wang *et al.* have reported on block or graft copolymers at the blending interface by reactive blending of methylene-diphenyl diisocyanate (MDI) and PLA in the melting state.[23] This strategy was used to improve the compatibility of PLA and starch. Liu *et al.* prepared super tough polymers by using reactive blending techniques. Cross-linked polyurethane (CPU) can be polymerized *in situ* by poly (ethylene glycol) (PEG) and polymeric methylene-diphenyl diisocyanate (PMDI) in PLA substrates. The interfacial compatibility between CPU and PLA could be achieved by the reaction of isocyanate (NCO) in CPU and the terminal hydroxyl groups in PLA. The impact strength and elongation at break of the reactive blending products were 20 to 30 times higher than that of the pristine PLA.[24] Zhu and his coworkers fabricated Poly (lactic acid-*co*-glycolic acid)/Polyurethane blended materials by chloroform casting. The results indicated that the addition of polyurethane (PU) significantly

improved the performance of PLGA films due to the reactive blending.[25] However, there are two disadvantages which limited their applications: (1) The massive addition of polymers like polyurethane significantly increased the cost of the blending materials; (2) The use of organic solvent inevitably polluted the environment. Furthermore, the analysis of the interfacial interaction between PLA matrix and PU is important to understand the structure of the PLA blend. Therefore, a highly efficient and environment-friendly polymer with low cost is needed to improve the performance of PLA with reactive blending.

Owing to the highly reactive isocyanate groups, polyurethane prepolymer (PUP) has attracted intensive attention.[26] Our previous studies showed that polyurethane microspheres are formed from PUP under high shear force, and the polyurethane microspheres could reactively blend with polymers having hydroxyl groups. With brittle materials such as starch and silk protein, prominent plasticization was achieved with low content of the PUP.[27–31] PUPs were exposed to moisture to completely terminate the NCO groups in PUP, milled in liquid nitrogen to prepare PU powder. The PU powder was then mixed with a polymer matrix to prepare an important control sample for clear analysis of the interface structure of the blends.

In this work, the plasticizer PUP was prepared by the reaction of Poly-1,4-butylene glycol adipate diol (PBA) dihydric alcohol and MDI, and then PLA/PUP blended materials were prepared by the reactive blending method using PLA and a small amount of PUP. In addition, PLA was blended with PU powder to obtain a control for analyzing the interface structure of the blends. The plasticization effects of PUP on PLA and the detailed microstructures and performance of the polymer blends were investigated.

EXPERIMENTAL

Materials

PLA 3032D was purchased from Nature Works LLC (USA). Poly-1,4-butylene glycol adipate diol (PBA diol, $M_w = 1000$ g mol^{-1}) was purchased from Yutian Chemical Industry (Jiangxi, China). 4,4′-Methylenedi-*p*-phenyl diisocyanate (MDI, 98%) was purchased from Sigma-Aldrich Fine Chemicals (St. Louis, MO).

Synthesis of Polyurethane Prepolymer (PUP)

The molar number ratio of isocyanate to hydroxyl group (NCO/OH) was 2.0. PBA diol (160 g) was added into a 250 mL three-necked flask fitted with a stirrer operating at a speed of 300 rpm, an inlet and an outlet. The system was vacuum dried (2 mmHg) at 110°C to remove the moisture in the PBA diol. After 30 min, the temperature of PBA diol in the flask was decreased to 70°C, and then MDI (80 g) was added in the flask under a nitrogen atmosphere. The translucent mixture in the flask quickly became transparent. Fifteen minutes after the addition of MDI, the mixture was stirred vigorously and left to react at 80°C for 1 h. A transparent white PUP was finally obtained.

Preparation of PU Powder

PU powder (PW) here was a control sample for PUP. PUP was poured into a mold and cured under ambient conditions for 30 days in order to prepare a PU sheet. In this case, the unreacted terminal NCO groups of the PUP were consumed by moisture in air. The PU sheet was milled into PU powder in polymer grinder (GP-00001 model, Wuhan Qien Science & Technology, Wuhan, China) using liquid nitrogen. The PU powder was then filtered using an 80 mesh screen.

Preparation of the PLA/PUP Blends

PLA (71.25 g) and PUP (3.75 g) were added into an intensive mixer (SU-70, Changzhou Suyan Science and Technology, Changzhou city, China) and mixed reactively at 160°C with a stirrer speed of 100 rpm. After 10 min, a white PLA/PUP blend was obtained. The PLA/PUP blend was equilibrated in a sealed plastic bag for 1 day before use. The blend consisting of PLA (95 wt %) and PUP (5 wt %) was designated as PLAPU. As a control, the same amount of PW was mixed with PLA by the same procedure, and the resulting mixture was designated as PLAPW.

Preparation of Sample Sheets by Compression-Molding

PLA/PUP blends were compression-molded in a hot press (R3202 model, Wuhan Qien Science & Technology, Wuhan, China) equipped with a water cooling system. The molding time, temperature and pressure were 5 min, 160°C and 40 MPa, respectively. The sheets were cut into a dumbbell-like sheet (5A type) according to GB/T1040-2006. The length of the dumbbell-like sheet was 75 mm, and width of the narrow section was 4 mm.

Fourier Transform Infrared Spectroscopy (FTIR)

A Fourier transform infrared spectrometer with an attenuated total reflectance (ATR FT-IR) accessory was used for qualitative investigation of the PLA/PUP blend. The sheet sample was placed in direct contact with the probe on a Nicolet 8700 FTIR spectrometer (Thermo Fisher Scientific, Surrey, UK). The measurement range was 4000–400cm^{-1} and the FTIR spectra were obtained using a resolution of 4 cm^{-1}. Each spectrum represented 64 added scans whose ratio was calculated against a reference spectrum obtained by recording 64 scans of an empty cell.

Emission Scanning Electron Microscopy (ESEM)

An ESEM (FEI, Quanta 200 FEG, Netherlands) was used to observe the cross-sections of fractured samples. Each sample was frozen using liquid nitrogen, and then fractured using tweezers to produce cross-sections. The cross-sections were then coated with gold and used for ESEM observation.

Differential Scanning Calorimetry (DSC)

DSC experiments (Diamond DSC, PerkinElmer Instruments, MA) were conducted in a nitrogenous atmosphere. The system was calibrated with indium and about 10 mg of the sample was placed in an aluminum pan and sealed. The samples were stabilized at 30°C for 1 min before they were heated to 200°C at 10°C min^{-1} and then the samples were held at 200°C for 5 min to erase thermal history prior to cooling down to 30°C at 25°C min^{-1}. After 1 min at 30°C, the second scan from 30°C to 200°C at 10°C min^{-1} was performed. The T_g was determined on the second scan at the midpoint of the calorific capacity change on the thermogram.

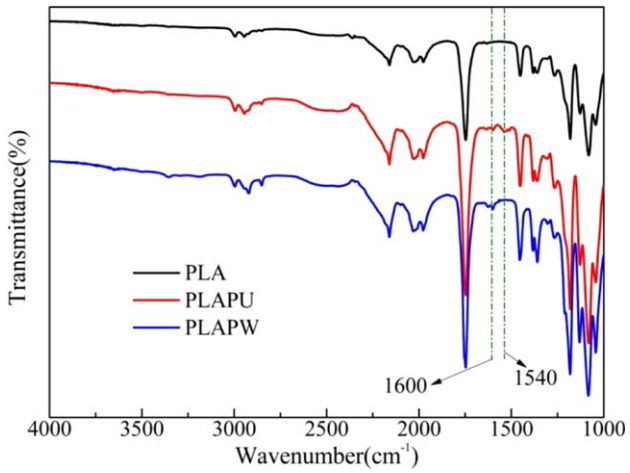

Figure 1. FTIR spectra of PLA, PLAPU, and PLAPW. [Color figure can be viewed in the online issue, which is available at wileyonlinelibrary.com.]

Dynamic Mechanical Properties (DMA)

Thermo-mechanical properties of the sheets obtained by compression-molding were tested in the solid state with a dynamic mechanical analyzer (DMA Q800, TA Instruments, USA) in a tensile mode. Tests were performed from −70 to 130°C at a heating rate of 5°C min^{-1} and an oscillation frequency of 1 Hz.

Thermal Gravimetric Analysis (TGA)

Testing was conducted using a thermal gravimetric analyzer (STA 449C, NETZSCH Instruments Inc., MA, USA). Approximately 10 mg of the sample cut from the sheet was equilibrated at ambient conditions and then subjected to heating from 30 to 700°C at a rate of 10°C min^{-1} in a nitrogen atmosphere. The weight loss with respect to temperature and the maximum degradation temperature (T_{max}) of samples were recorded.

Tensile Test

Mechanical properties were measured using a tensile tester (CMT6503, Shenzhen SANS Test Machine) according to ASTM D 882-81 with a strain rate of 5 mm min^{-1}. The distance between the two clamps was 40 mm. Strength at break (σ_b, MPa) and elongation at break (ϵ_b, %) of the sheets were recorded. Five duplications were made.

RESULTS AND DISCUSSION

Structure

Figure 1 shows the FTIR spectra of PLA, PLAPU, and PLAPW. All the characteristic absorption peaks of PLA were observed in the FTIR spectra of the PLAPU. As shown in the spectrum of PLAPU, two new characteristic absorption peaks were observed at 1540 and 1600 cm^{-1}. The peak at 1,540 cm^{-1} was attributed to the urethane bonds,[23] and the peak at 1600 cm^{-1} corresponded to the conjugated double bonds of benzene.[32] These two peaks indicated the occurrence of *in situ* reactions between the NCO groups in the PUP and the terminal hydroxyl or carboxyl groups in PLA. Moreover, the absence of the characteristic absorption peak of NCO in PUP at 2295 cm^{-1} in the FITR spectrum of PLAPU indicated the complete consumption of the NCO in PUP during the reactive blending.[33] To further verify that the urethane bonds formed during the blending process originated from the terminal reactions between PLA and PUP, PLAPW was also analyzed. In the spectrum of PLAPW, no characteristic absorption peak at 1540 cm^{-1} corresponding to the urethane bonds was observed, meanwhile the conjugated double bonds of benzene at 1600 cm^{-1} were present, indicating that the PW did not react with the terminal hydroxyl or carboxyl groups in PLA during the blending process. Therefore, during the blending of PLA with PUP, the terminal hydroxyl or carboxyl groups in PLA reacted *in situ* with the NCO groups in PUP.

Figure 2 shows the cross-sectional SEM images of PLA, PLAPU, and PLAPW after the treatment with liquid nitrogen. As shown in Figure 2(a), PLA shows a smooth and sharp cross section with no observed phase separations, indicating that PLA is a brittle material. In contrast, a rough surface was observed for the PLAPU blend as shown in Figure 2(b). The fact that the PU micro-particles were uniformly distributed in the PLA substrate suggested that the PU micro-particles were formed during the blending of PLA and PUP. Again, no cavities and cracks were observed at the interface between PUP and PLA, indicating an excellent compatibility between PUP and PLA. The compatibility was as a result of the strong urethane linkage between the PU micro-particles and PLA matrix. In comparison with Figure 2(c), the PW were pulled out of their domains from the PLA substrate during the rupture process, and many cavities were clearly observed, this is because there were no reactivity and

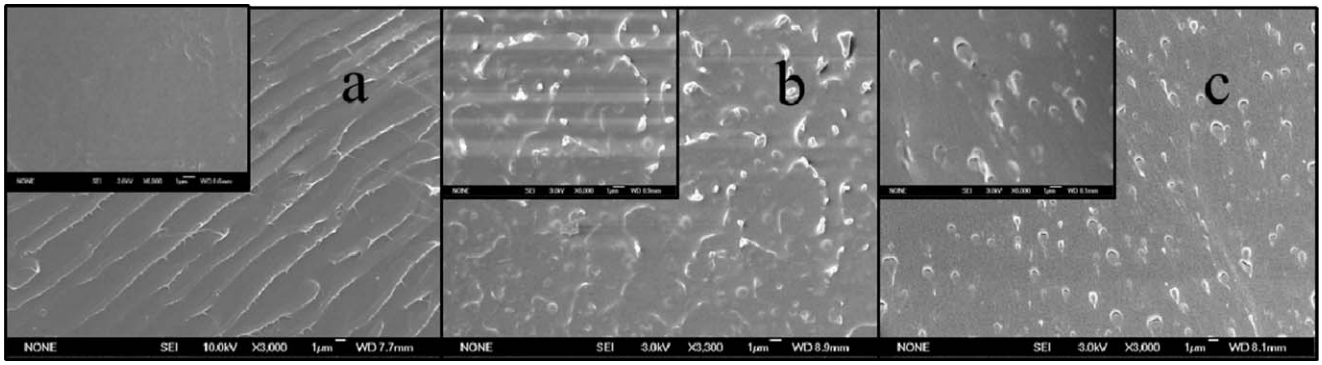

Figure 2. SEM micrographs of PLA, PLAPU, and PLAPW.SEM images of: a) PLA (10.0KV, ×3000); b) PLAPU (3.0KV, ×3300); c) PLAPW (3.0KV, ×3000).

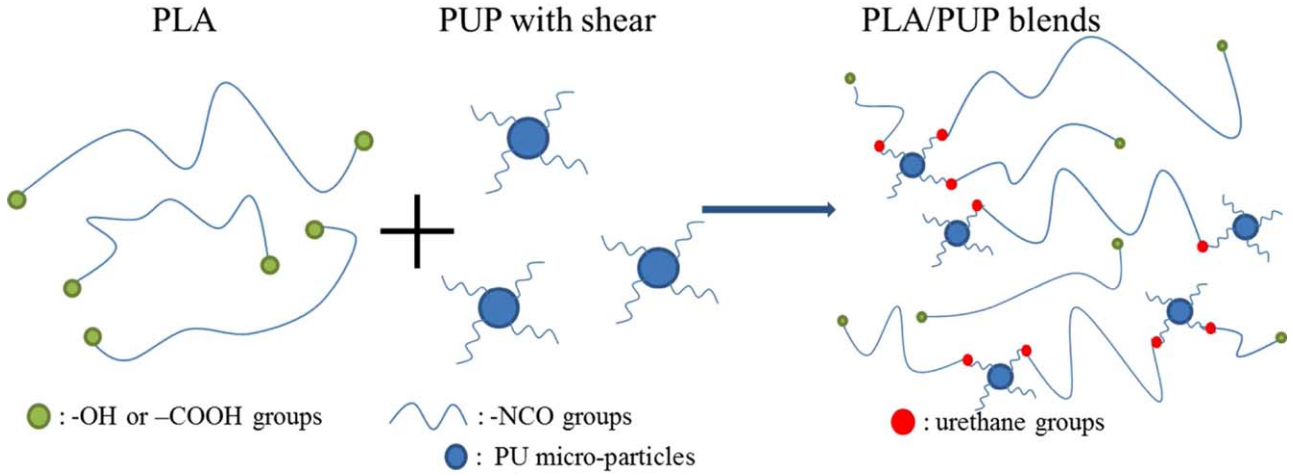

Figure 3. Schematic diagram of PLA/PUP blends. [Color figure can be viewed in the online issue, which is available at wileyonlinelibrary.com.]

compatibility between PW and PLA. The results further indicated that an interface with excellent compatibility can be prepared by the reactions of the terminal hydroxyl or carboxyl groups in PLA and the NCO groups in PUP during reactive blending.

Based on these results, a schematic diagram for the reactive blending of PLA and PUP is shown in Figure 3. The urethane bonds formed by the reactions between the terminal hydroxyl or carboxyl groups and the NCO groups in PUP promoted the uniform distribution of the PU micro-particles in the PLA substrate.

Thermal Properties

Figure 4 shows the DSC curves of PLA, PLAPU and PLAPW. An obvious glass transition peak of PLA was observed at 63.7°C.[34] After blending PLA with PUP, this peak shifted to 61.9°C in PLAPU because of the low glass transition temperature of PUP. Thus, the addition of PUP slightly decreased the total glass transition temperature of PLA. In contrast, the glass transition temperature of PLAPW was found to be 63.8°C, which is similar to that of the pristine PLA, indicating that the PW was incompatible with PLA. As a result, the addition of PW did not affect the glass transition temperature of PLA. Therefore, a prominent compatibility was achieved by the reactive blending of PUP and PLA. Furthermore, a crystalline melting peak was observed on the DSC curve. The pristine PLA had T_{cc} at 117°C. After PUP was added, the T_{cc} shifted to a lower temperature indicating that, the PUP accelerated the crystallization process of PLA. As shown in Table I, the heat of melting (ΔH_m) and the heat of cold crystallization (ΔH_{cc}) were decreased after the PUP was added, suggesting that the addition of PUP decreased the crystallinity of PLA.

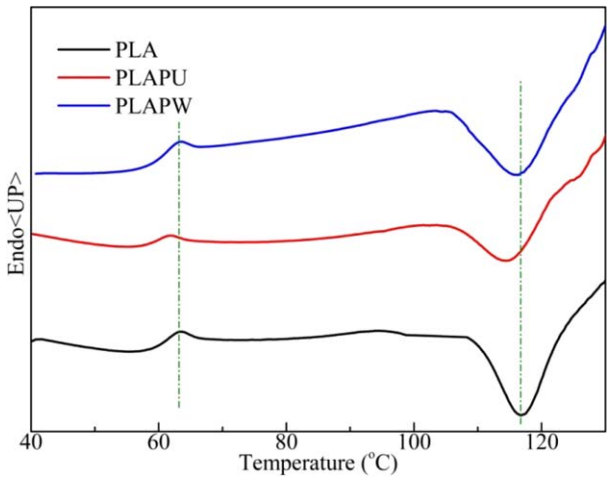

Figure 4. DSC thermogram for PLA, PLAPU, and PLAPW. [Color figure can be viewed in the online issue, which is available at wileyonlinelibrary.com.]

Figure 5 shows the Tan δ and storage modulus (E') curves of PLA, PLAPU and PLAPW. As shown in the storage modulus curves, the intensity of PLAPU was lower than that of the pristine PLA at the temperatures before T_g, and this could be attributed to the lower rigidity of PLA caused by the addition of PUP. The two obvious slopes in PLAPU corresponded to the T_g of the PUP soft segment and the T_g of the PLA substrate.[35,36] In contrast, only one slope corresponding to the T_g was observed in PLA. Similarly, two obvious T_g peaks corresponding to PLA and PUP soft segment in the Tan δ curve of PLAPU were observed while only one T_g peak was observed in the pristine PLA. The T_g of PLAPU was lower than that of the pristine PLA, and the same results were also obtained from the DSC analysis, which could be explained by the plasticization effect of PUP. However, the storage modulus intensity of the control sample PLAPW was higher than that of PLA and PLAPU before

Table I. Melting and Crystallization Properties of PLA, PLAPU, and PLAPW

Sample	T_g (°C)	ΔH_m (J/g)	T_{cc} (°C)	ΔH_{cc} (J/g)
PLA	63.7	32.5	117.9	58.7
PLAPU	61.9	26.2	112.4	38.9
PLAPW	63.8	30.9	116.1	43.8

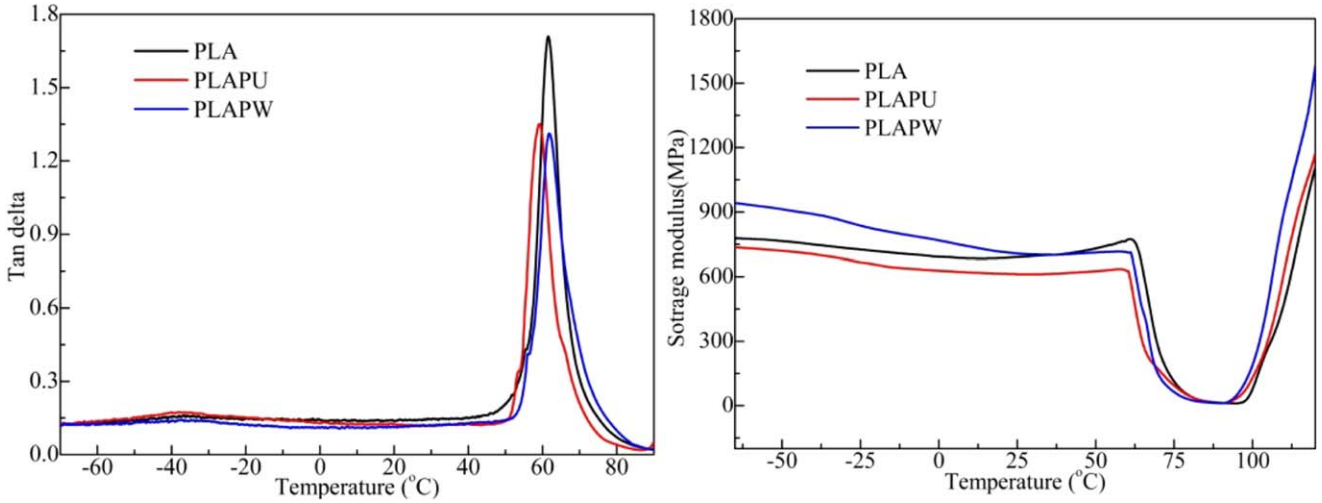

Figure 5. Tan δ and storage modulus (E') curves of PLA, PLAPU, and PLAPW. [Color figure can be viewed in the online issue, which is available at wileyonlinelibrary.com.]

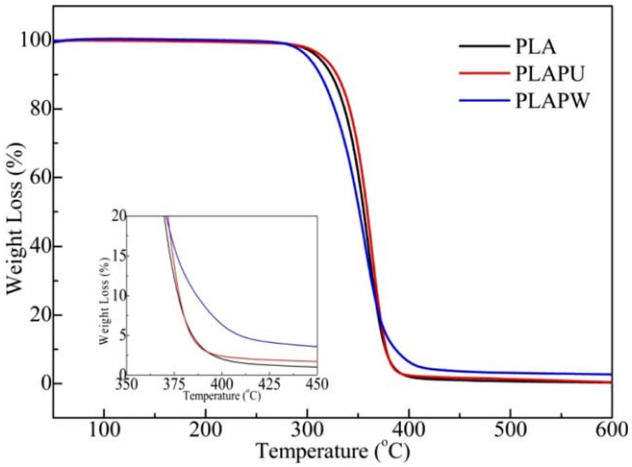

Figure 6. TGA thermograms of PLA, PLAPU, and PLAPW. [Color figure can be viewed in the online issue, which is available at wileyonlinelibrary.com.]

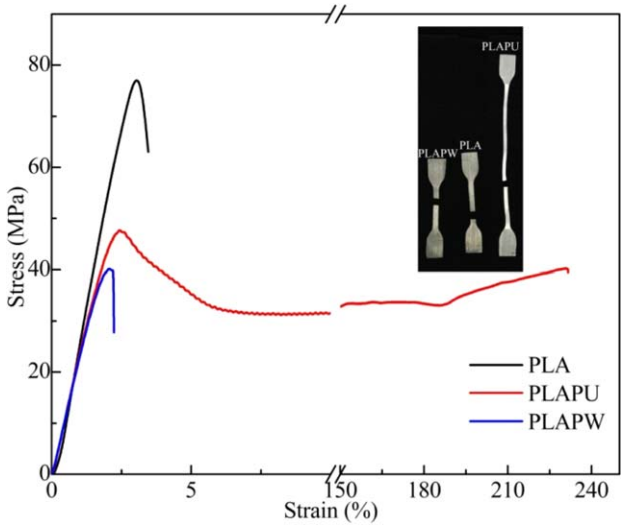

Figure 7. Stress−strain curves of PLA, PLAPU, and PLAPW. [Color figure can be viewed in the online issue, which is available at wileyonlinelibrary.com.]

T_g because the PW was a thermoset, showing more stiffness than the PU in PLAPU. In addition, the obtained Tan δ and storage modulus for PLAPW were similar to that of the pristine PLA, indicating no compatibility between the PLA and the PW. Therefore, the NCO groups were considered to have played a key role in the PLA/PUP blending.

The thermal stability of PLAPU was also evaluated by TGA. Figure 6 shows the TGA curves of PLA, PLAPU, and PLAPW. A drastic weight loss of all the samples was observed in the range of 300 − 400°C because of the thermal decomposition of PLA

Table II. Formulations and Tensile Properties of the PLA, PLAPU, and PLAPW

	Formulation of the modification		Properties of the molded sheets		
Sample	PLA(g)	PU(g)	σb(MPa)	εb(%)	*E*(Mpa)
PLA	75	0	72.4 ± 2.1	2.9 ± 0.1	3173.7 ± 129.7
PLAPU	71.25	3.75	44.9 ± 3.1	231.5 ± 9.5	2798 ± 117.3
PLAPW	71.25	3.75(PW)	39.8 ± 1.5	1.8 ± 0.2	2835 ± 100.5

substrate.[37] The residual weight of PLAPU which was much higher than that of PLA in the range of 400 − 500°C was attributed to the higher decomposition temperature of the PUP soft segment in PLAPU.[38] However from 500°C, the residual weights of PLAPU and PLA were approximately the same. Again, from the TGA curves, the highest decomposition temperatures of PLA and PLAPU were 359.3°C and 362.6°C, respectively. These results indicated that the urethane bonds formed improved the thermal stability of PLAPU. Moreover, the highest decomposition temperature of PLAPW was lower than that of PLA because the PLA in PLAPW was not bound with the PU dispersion phase. The MDI hard domains in the composition of PLAPW were hardly decomposed because the unreacted MDI were cross-linked during mixing. As a result, PLAPW had a higher residual weight than those of PLAPU and PLA from 400°C. These experiments clearly showed that the thermal stability of the PLA was improved by the reactive blending with PUP.

Mechanical Properties

Figure 7 shows the stress−strain curves of PLA, PLAPU, and PLAPW, and Table II lists the detailed results. The elongation ratio at break for the pristine PLA was 2.9%; however, it did not show any yield. The obvious yield and neck stretch were obtained after the addition of PUP, and the elongation ratio at break increased from 2.9% to 231.5%. In contrast, the mechanical properties of PLAPW decreased significantly mainly due to the simple physical blending of the polymers without the formation of covalent bonds. The incompatibility between PLA and PW resulted in the decreased tensile properties of PLAPW. Therefore, a lower content of PUP could significantly improve the mechanical prperties of PLA by the reactive blending of PLA and PUP.

CONCLUSIONS

In this study, PUP was prepared by the reaction of PBA dihydric alcohol and MDI. Subsequently, the ensuing PUP was reactively blended with PLA. The PLAPW as a control sample proved that there was no reaction between PLA and PU powder which indicated that the NCO groups in PUP were the key to the reactive blending. The results of the FTIR, SEM, DSC, and DMA analysis indicated that the reaction between the NCO groups in PUP and the terminal hydroxyl or carboxyl groups in PLA significantly improved the compatibility between the PUP and the PLA. Compared to pristine PLA, the highest decomposition temperature of PLAPU increased from 359.3°C to 362.6°C, and the elongation ratio at break rose from 2.9% to 231.5%. The thermal stability and mechanical properties of the blended materials were exceedingly improved even with 5% of PUP in the blended materials. These results further indicated that a lower content of PUP can significantly improve the properties of PLA by the reactive blending method.

ACKNOWLEDGMENTS

The authors would like to express their appreciation for the financial support from the National Natural Science Foundation of China under grant No. 50803024.

REFERENCES

1. Anderson, K. S.; Schreck, K. M.; Hillmyer, M. A. *Polym. Rev.* **2008**, *48*, 85.
2. Tschan, M. J. L.; Brul, E.; Haquette, E.; Thomas, P. C. M. *Polym. Chem.* **2012**, *3*, 836.
3. Rasal, R. M.; Janorkar, A. V.; Hirt, D. E. *Prog. Polym. Sci.* **2010**, *35*, 338.
4. Xiong, Z.; Zhang, L. S.; Ma, S. Q.; Yang, Y.; Zhang, C. Z.; Tang, Z. B.; Zhu, J. *Carbohydr. Polym.* **2013**, *94*, 235.
5. Concetaa, G.; Isaac, A.; John, T. *Colloid. Surface B* **2013**, *112*, 9.
6. Auras, R.; Harte, B.; Selke, S. *Macromol. Biosci.* **2004**, *4*, 835.
7. Wei, Z.; Song, P.; Zhou, C.; Chen, G.; Chang, Y.; Li, J. *Polymer* **2013**, *54*, 3377.
8. Qiu, J. S.; Xing, C. Y.; Cao, X. J.; Wang, H. T.; Wang, L.; Zhao, L. P.; Li, Y. *J. Macromol.* **2013**, *46*, 5806.
9. Odent, J.; Leclère, P.; Raquez, J. M.; Dubois, P. *Eur. Polym. J.* **2013**, *49*, 914.
10. Simoes, C. L.; Viana, J. C.; Cunha, A. M. *J. Appl. Polym. Sci.* **2009**, *112*, 345.
11. Jun, W. P.; Seung, S. I. *Polymer* **2003**, *44*, 4341.
12. Baiardo, M.; Frisoni, G.; Scandola, M.; Rimelen, M.; Lips, D.; Ruffieux, K.; Wintermantel, E. *J. Appl. Polym. Sci.* **2003**, *90*, 1731.
13. Imre, B.; Bedó, D.; Domjánd, A.; Schönd, P.; Vancso, G. J.; Pukánszky, B. *Eur. Polym. J.* **2013**, *49*, 3104.
14. Gua, S. Y.; Zhang, K.; Ren, J.; Zhan, H. *Carbohydr. Polym.* **2008**, *74*, 79.
15. Kang, H. L.; Qiao, B.; Wang, R. G.; Wang, Z.; Zhang, L. Q.; Ma, J.; Coastes, P. *Polymer* **2013**, *54*, 2450.
16. Harada, M.; Ohya, T.; Iida, K.; Hayashi, H.; Hirano, K.; Fukuda, H. *J. Appl. Polym. Sci.* **2007**, *106*, 1813.
17. Feng, F.; Ye, L. *J. Appl. Polym. Sci.* **2011**, *119*, 2778.
18. Han, J. J.; Huang, H. X. *J. Appl. Polym. Sci.* **2011**, *120*, 3217.
19. Meredith, J. C.; Amis, E. *J. Chem. Phys.* **2000**, *201*, 733.
20. Oyama, H. T.; Inoue, T. *Macromolecules* **2001**, *34*, 3331.
21. Oyama, H. T.; Kitagawa, T.; Ougizawa, T.; Inoue, T.; Weber, M. *Polymer* **2004**, *45*, 1033.
22. Macosko, C. W.; Jeon, H. K.; Hoye, T. R. *Prog. Polym. Sci.* **2005**, *30*, 939.
23. Wang, H.; Sun, X. Z.; Seib, P. *J. Appl. Polym. Sci.* **2001**, *82*, 1761.
24. Liu, G. C.; He, Y. S.; Zeng, J. B.; Xu, Y.; Wang, Y. Z. *Polym. Chem.* **2014**, *5*, 2530.
25. Zhu, G. Q.; Wang, F. G.; Tan, H. S.; Gao, Q. C.; Liu, Y. Y. *Chem. Pap.* **2014**, *68*, 246.
26. Yang, H. Y.; Wang, X.; Yu, B.; Yuan, H. X.; Song, L.; Hu, Y.; Yuen, R. K. K.; Yeoh, G. H. *J. Appl. Polym. Sci.* **2013**, *128*, 2720.

27. Wu, Q. X. Pat., CN101100531A, **2008**.
28. Wu, Q. X.; Wu, Z. S.; Tian, H. F.; Zhang, Y.; Cai, S. *Ind. Eng. Chem. Res.* **2008**, *47*, 9896.
29. Wu, Q. X.; Chen, X. X.; Zhang, Y.; Wu, Z. S.; Huang, Y. *Ind. Eng. Chem. Res.* **2011**, *50*, 2008.
30. Wei, M.; Hyang, Y.; Zhang, Y.; Chen, X. X.; Wu, Z. S.; Wu, Q. X. *J. Biobased Mater. Bio.* **2011**, *5*, 1.
31. Zhang, Y.; Zhang, P. P.; Chen, X. X.; Wu, Z. S.; Wu, Q. X. *Ind. Eng. Chem. Res.* **2011**, *50*, 2111.
32. Chen, X.; Gardella, J. A.; Ho, T.; Wynne, K. J. *Macromolecules* **1995**, *28*, 1635.
33. Sultana, M.; Bhattia, H. N.; Zuberb, M.; Bhattia, I. A.; Sheikha, M. A. *Carbohydr. Polym.* **2001**, *86*, 928.
34. Migliaresi, C.; Cohn, D.; De, L. A.; Fambri, L. *J. Appl. Polym. Sci.* **1991**, *43*, 83.
35. Martin, O.; Averous, L. *Polymer* **2001**, *42*, 6237.
36. Menard, K. P. The Chemical Rubber Company Press: Boca Raton **1999**.
37. Tomoko, S.; Yoichi, K.; Hironori, M.; Yoichi, T.; Shigeo, A.; Masao, S. *Polymer* **2006**, *47*, 4839.
38. Liao, J. J.; Luo, Z. M.; Zhang, Y.; Zhang, X.; Cheng, J.; Wu, Q. X. *New J. Chem.* **2014**, *38*, 2522.